Temporal niche differentiation of parasites sharing the same plant host: oak powdery mildew as a case study

Frédéric Marie Hamelin, Anne Bisson, Marie-Laure Desprez Loustau, Frédéric Fabre, Ludovic Mailleret

esa

ECOSPHERE

Temporal niche differentiation of parasites sharing the same plant host: oak powdery mildew as a case study

Frédéric M. Hamelin,[1,†] Anne Bisson,[2,3] Marie-Laure Desprez-Loustau,[4] Frédéric Fabre,[5] and Ludovic Mailleret[6,7]

[1]*IGEPP, Agrocampus Ouest, INRA, Université de Rennes 1, Université Bretagne-Loire, 65 rue de Saint Brieuc, 35000 Rennes, France*
[2]*INRA, UMR 0729 MISTEA, 2 Place Pierre Viala, 34060 Montpellier, France*
[3]*INRA, UMR 1222 Eco&Sols, 2 Place Pierre Viala, 34060 Montpellier, France*
[4]*INRA, UMR 1202 BIOGECO, 69 Route d'Arcachon, 33612 Cestas, France*
[5]*INRA, UMR 1065 SAVE, 71, Avenue Edouard Bourlaux, 33882 Villenave d'Ornon, France*
[6]*Université Côte d'Azur, INRA, CNRS, ISA, 400 route des chappes, Sophia Antipolis, France*
[7]*Université Côte d'Azur, Inria, INRA, CNRS, UPMC Univ Paris 06, 2004 route des lucioles, Sophia Antipolis, France*

Citation: Hamelin, F. M., A. Bisson, M.-L. Desprez-Loustau, F. Fabre, and L. Mailleret. 2016. Temporal niche differentiation of parasites sharing the same plant host: oak powdery mildew as a case study. Ecosphere 7(11):e01517. 10.1002/ecs2.1517

Abstract. Plant diseases are often caused by complexes of closely related parasite species. The coexistence of species sharing the same niche challenges the competitive exclusion principle. Here, we performed the mathematical analysis of a generic model of sibling parasite species coexistence based on seasonality. We showed that coexistence through temporal niche partitioning is biologically plausible as it occurred in a significant part of the parameter space of the model. Moreover, the reversal of species relative frequencies (i.e., the most frequent species at the beginning of the season becoming the last frequent at the end) can occur without compromising the long-term coexistence of the two species. We provided data showing that this reversal pattern does repeat over years in the case of two sibling species responsible for oak powdery mildew (*Erysiphe alphitoides* and *Erysiphe quercicola*) in Europe. Last, the model was fitted to the data and satisfactorily described the population dynamics of oak powdery mildew species. The seasonal succession of these two plant pathogen species provides one of the few examples of coexistence by temporal niche partitioning at the scale of the season caused by exploitative competition. We discuss whether evolutionary branching may have led to temporal niche differentiation in this system.

Key words: coexistence; epidemiology; pathogen; seasonality; semidiscrete model; trade-off.

Received 26 March 2016; revised 15 June 2016; accepted 21 June 2016. Corresponding Editor: Debra P. C. Peters.

† **E-mail:** fhamelin@agrocampus-ouest.fr

Introduction

Many widespread fungal plant diseases have long been attributed to a unique parasite species. Yet the advent of DNA sequence-based species identification techniques and the application of the phylogenetic species concept (Taylor et al. 2000) has led to the increasing recognition that many current names of common fungal plant diseases mask complexes of sibling species (Fitt et al. 2006). Such coexistence of closely related species that apparently occupy the same niche (the same host plant, and even the same organ) challenges the competitive exclusion principle (Gause 1934, Hardin 1960, Hutchinson 1961, Armstrong and McGehee 1980).

Among several hypothetic processes resolving this apparent paradox (Fitt et al. 2006), it was recently shown that a trade-off between transmission during the growing season and survival

during the off-season may theoretically allow sibling parasite species to coexist through temporal niche partitioning (Hamelin et al. 2011). Moreover, the two species may significantly overlap in time without compromising the coexistence (Kisdi 2012, Mailleret et al. 2012).

Although temporal niche partitioning is a commonly accepted concept, few examples clearly support it (Morin 2011, Shimadzu et al. 2013). The most convincing examples concern interference competition (occurring directly between individuals; Carothers and Jaksić 1984) and day–night cycles (Ziv et al. 1993, Albrecht and Gotelli 2001, Jones et al. 2001, Kronfeld-Schor and Dayan 2003, Adam and Thibault 2006, Valeix et al. 2007, Castro-Arellano and Lacher 2009, Di Bitetti et al. 2009, Harrington et al. 2009, Hayward and Slotow 2009). For example, Stuble et al. (2013) showed that within a deciduous forest ant community, "ant species appear to temporally partition foraging times such that behaviorally dominant species foraged more intensely at night, while foraging by subdominant species peaked during the day." Rarer still are examples of temporal niche partitioning at the scale of the season and through exploitative competition (occurring indirectly through a common limiting resource; Loreau 1989, Koide et al. 2007, Winder 2009, Harabiš et al. 2012).

However, an empirical study with plant pathogen fungi suggested temporal niche partitioning between two sibling species (Feau et al. 2012), as described in Hamelin et al. (2011). *Erysiphe alphitoides* and *Erysiphe quercicola* both cause oak powdery mildew, a major disease of oaks in Europe, but with contrasted seasonal dynamics. More specifically, Feau et al. (2012) reported a striking annual pattern: the reversal of the species relative frequencies during the season, hereafter the reversal pattern. Namely, *E. quercicola* was the first observed in spring, while *E. alphitoides* was dominant at the end of the season.

The aim of this study was (1) to explore whether coexistence of sibling pathogen species through temporal niche partitioning is biologically meaningful, that is, whether coexistence occurs in a significant part of the parameter space of the generic model of species coexistence (Hamelin et al. 2011); (2) to theoretically explore whether the reversal pattern in species frequencies during the season can occur without compromising long-term coexistence, which may seem unintuitive; (3) to test whether the reversal pattern is recurrent across years in the oak powdery mildew system (Feau et al. 2012) and to fit the model to the time series of oak powdery mildew.

Materials and Methods

Model

We focus on a fungal leaf parasite to make explicit assumptions and to later parameterize the model, but we keep the model as simple as possible for the sake of generality. A semidiscrete model (Mailleret and Lemesle 2009) describing the plant disease dynamics over many seasons is formulated. It includes primary and secondary infections. Primary infections refer to leaf infections originating from the fungus survival forms and initiating new epidemics in spring. Infected leaves produce infectious short-lived airborne spores. Secondary infections refer to leaf-to-leaf infections generating the epidemic phase during the season. To keep the model simple, we assume that the total leaf density is a constant all along the season. A continuous-time model is used to model disease transmission during the season. At the end of the season, leaves fall to the ground. The parasite switches to a survival form. The beginning of the next year is after buds have germinated and produced new shoots. The annual cycle repeats.

Let S and I be the densities of susceptible and infected leaves, respectively. More specifically, we let $I = I_1 + I_2$ with I_1 and I_2 representing leaves infected by species 1 or by species 2, respectively (we ignore multiple infections at the leaf scale). Let T be the duration of an annual cycle (1 yr) and n be a cycle index. Also, let τ be the length of the growing season (i.e., plants with living leaves), hereafter the season. Let β_1 and β_2 be the secondary infection rates, proportional to the number of infectious spores produced per infected leaf per unit time, associated with species 1 and species 2, respectively. Let α be the frequency at which infected leaves are removed from the epidemiological dynamics (e.g., defoliated).

During the season, that is, for all t between nT and $nT + \tau$, the epidemiological dynamics are governed by a SIR model (Kermack and McKendrick 1927, Segarra et al. 2001). For $i = 1$, 2, the model reads:

$$\begin{aligned}\frac{dS}{dt} &= -S(\beta_1 I_1 + \beta_2 I_2),\\ \frac{dI_i}{dt} &= I_i(\beta_i S - \alpha)\end{aligned}. \quad (1)$$

From season to season, that is, from $nT + \tau$ to $(n+1)T$, the dynamics are governed by a discrete-time model. Let S_0 be the initial susceptible host density (which is assumed to be renewed each year regardless of disease incidence) and χ_i be a composite parameter aggregating survival forms production per infected leaves, their survival probability, and their primary infection rate (Mailleret et al. 2012). This parameter is specific to each species and will be referred to as the between-season transmission parameter of species i. Assuming that primary infections occur on a shorter timescale than secondary infections, we consider the following: for $i = 1, 2$,

$$\begin{aligned}S((n+1)T) &= S_0 \exp\left(-\sum_{i=1}^{2} \chi_i I_i(nT+\tau)\right),\\ I_i((n+1)T) &= S_0\left(1-\exp\left(-\sum_{j=1}^{2} \chi_j I_j(nT+\tau)\right)\right)\\ &\quad \times \frac{\chi_i I_i(nT+\tau)}{\sum_{j=1}^{2} \chi_j I_j(nT+\tau)}\end{aligned} \quad (2)$$

The exponential term represents the probability for a susceptible leaf to escape primary infections. The fraction represents the probability to be infected by species 1 given that infection occurred. Table 1 is a list of the parameters and variables for model (1–2).

Table 1. Model parameters and variables.

Variable	Definition
n	Annual cycle index
t	Time (in year a)
$S(t)$	Susceptible leaf density (m^{-2})
$I(t)$	Infected leaf density (m^{-2})
$I_1(t)$	Infected by species 1 (m^{-2})
$I_2(t)$	Infected by species 2 (m^{-2})
τ	Length of the favorable season (≤ 1 a)
$T - \tau$	Length of the off-season (≤ 1 a)
β_1, β_2	In-season transmission rates (m^2/a)
χ_1, χ_2	Between-season infection zones (m^2)
α	Infected leaf removal rate (a^{-1})
S_0	Initial and maximal density (m^{-2})

Fig. 1 presents model (1–2) dynamics for a parameter set enabling coexistence of both species (Mailleret et al. 2012). To which extent coexistence is a generic phenomenon remained to be explored, as well as whether the reversal of the species relative frequencies can occur during the season. To address these issues, we performed a mathematical analysis, which is reported in Appendix S1: Section A.

Study system

Powdery mildew is a major disease of oaks in Europe. As in all powdery mildew diseases, typical symptoms are white powdery patches, which may cover the entire leaf surface, most commonly on the upper side. This white powder is constituted by the asexual spores of the fungus, which are produced from the mycelium running on the leaf surface. Powdery mildew fungi are obligate biotrophic parasites, which feed from their host's living cells using differentiated absorptive organs called haustoria (Glawe 2008). In temperate regions, they have a seasonal cycle as they cannot develop in the absence of susceptible host tissues (living leaves). Two overwintering modes have been described. The fungus may survive as mycelium within buds infected in the previous season, protected by bud scales. Else, chasmothecia, the sexual fruiting bodies produced in late summer on infected leaves, can act as surviving organs, kept dormant during winter. Primary inoculum in spring, initiating the annual epidemics, is then either constituted by flag shoots, that is, shoots arising from infected buds producing high numbers of conidiospores, or by ascospores, released by chasmothecia (Glawe 2008).

Although a few reports of oak powdery mildew had been made in the 19th century, the disease became prevalent only in the beginning of the 20th century, when severe epidemics suddenly appeared and rapidly spread all over Europe. The causal agent was shown to be a previously undescribed species of unknown origin and it was called *Erysiphe alphitoides* (Mougou et al. 2008). The disease mainly affects *Quercus robur* and *Q. petraea* and causes most damage in seedlings, coppice, or pruned trees and mature trees previously defoliated by frost or insects, where infections can lead

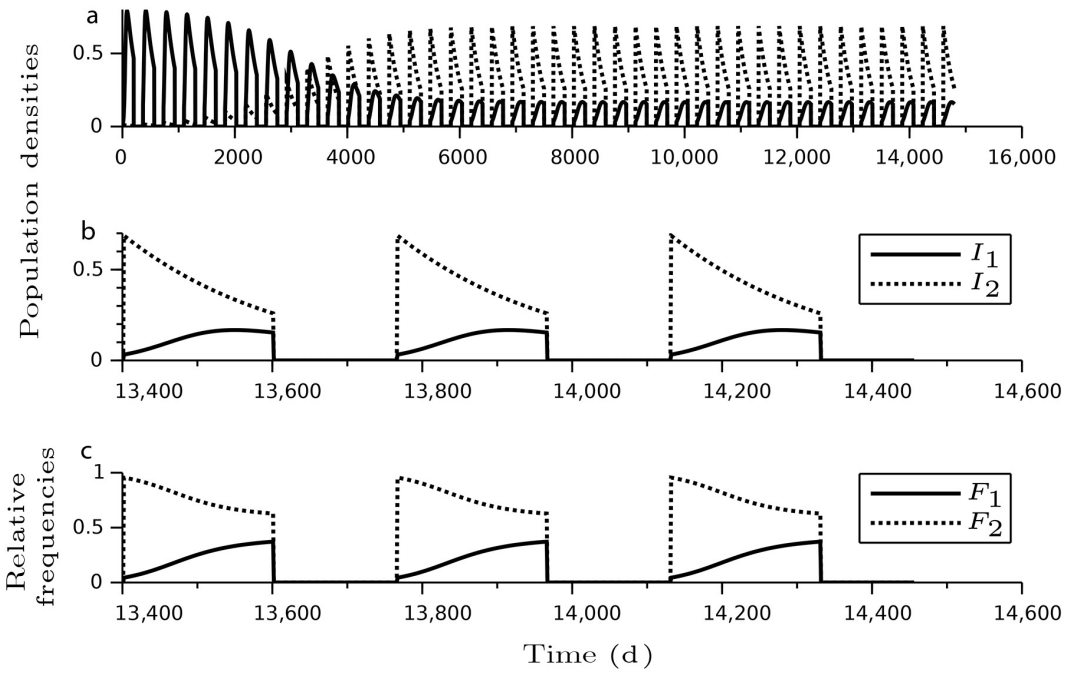

Fig. 1. Long-run coexistence without reversal of the species relative frequencies. Parameter values: $\alpha = 0.005$, $\beta_1 = 0.1$, $\beta_2 = 0.001$, $\chi_1 = 0.369$, $\chi_2 = 4.68$, $T = 365$, $\tau = 200$, and $S_0 = 1$. (a) Infected densities I_1 and I_2, for $n = 40$ cycles (yr). (b) Zoom on the last 3 cycles. (c) Species relative frequencies over the last 3 cycles; that is, for $i = 1, 2$, $F_i = I_i/(I_1 + I_2)$.

to mortality or decline (Marçais and Desprez-Loustau 2014). Recent studies using polymorphism of the ribosomal DNA demonstrated the occurrence of several cryptic species associated with oak powdery mildew symptoms (Mougou et al. 2008). Although *E. alphitoides* represented more than 80% of samples in a wide survey in France, the recently described *Erysiphe quercicola* (Takamatsu et al. 2007) was found in approximately 15% of samples. Based on its wide distribution all over the country, albeit at a low relative frequency in most locations (Mougou-Hamdane et al. 2010), *E. quercicola* has likely been present in Europe for several decades now. Moreover, Feau et al. (2012) showed a strict association between *E. alphitoides* with chasmothecia on the one hand and *E. quercicola* with flag shoots on the other hand. Recent phylogenetic studies on powdery mildews suggest that *E. alphitoides* and *E. quercicola* are closely related sibling species, included in a cluster that underwent speciation from a common ancestor on *Quercus* species, maybe in Eastern Asia (Takamatsu et al. 2007, 2015).

Data

A fine monitoring of the temporal dynamics of *E. alphitoides* (*E.a*) and *E. quercicola* (*E.q*) was performed in "Les sources" forest (Cestas, France) during year 2014 (from 18 April to 17 October). Powdery mildew was sampled from oak (*Quercus robur*) seedlings in two natural regeneration plots separated by a distance of 200 m (total sampled area: 14 m^2; approximate seedling oak density: 400 m^{-2}). On the first sampling date, all plants in the sampling plots were visually assessed for symptoms typical of powdery mildew. Only flag shoot symptoms were observed, and the initial proportion of diseased plants was $22/(400 \times 14) = 0.0039 \approx 4 \times 10^{-3}$. A small infected leaf fragment (0.5 × 0.5 cm) was cut out from each infected seedling and directly put in an Eppendorf tube and brought back to the laboratory for further analysis. Subsequent independent samplings were made at more or less weekly intervals, with 30 leaves (15 from each plot) showing oak powdery mildew symptoms sampled at each date as described earlier. The identification of powdery mildew species for

each leaf sample was based on ITS (nuclear ribosomal internal transcribed spacer) DNA sequences, the official barcoding region for fungi (Schoch et al. 2012, Appendix S1: Section B). Only single infections were considered for model fitting as mixed infection data are uninformative to estimate *E.a* and *E.q* relative frequencies (Appendix S1: Table S1). Data reported in the study by Feau et al. (2012) from a similar (less intensive) monitoring in the same area were also used (Appendix S1: Table S2; sampled area: 800 m^2; approximate seedling oak density: 20 m^{-2}; nine flag shoots). The initial proportion of diseased plants was $9/(800 \times 20) \approx 5.6 \times 10^{-4}$.

Independent data obtained from a large survey in France are also presented as an illustration (Fig. 2). In this case, samplings were performed both in natural oak regenerations (17 locations in 2012 and 23 in 2013) and young plantations (15 locations in 2012 and eight in 2013) representing most of the distribution area of oaks (*Q. robur* and *Q. petraea*) in France. Each stand (regeneration or plantation) was visited at two dates in the same year, in June and September. At each date, the prevalence of powdery mildew (% plants infected) was recorded on 30 plants per site taken at random on three 100 m long transects (according to methods used by the French Forest Health Department) and 10 infected leaves taken from different plants were sent to the laboratory for powdery mildew species identification (Appendix S1: Section B).

Mathematical reformulation

To compare model outputs with data (species relative frequencies and initial proportion of infected individuals), we let $F = I_1/I$, with $I = I_1 + I_2$. Following the mathematical analysis in Appendix S1: Section A, we neglected defoliation and restricted our attention to the case $\alpha = 0$, which implies that R is equal to zero so $S + I = N$ (the total leaf density, a constant). Also, we chose our space unit such that $N = 1$ without loss of generality. This yields $S = 1 - I$. Under these assumptions, model (1–2) is equivalent to: for all t between nT and $nT + \tau$,

$$\frac{dF}{dt} = (\beta_1 - \beta_2)F(1-F)(1-I),$$
$$\frac{dI}{dt} = (\beta_1 F + \beta_2(1-F))I(1-I), \quad (3)$$

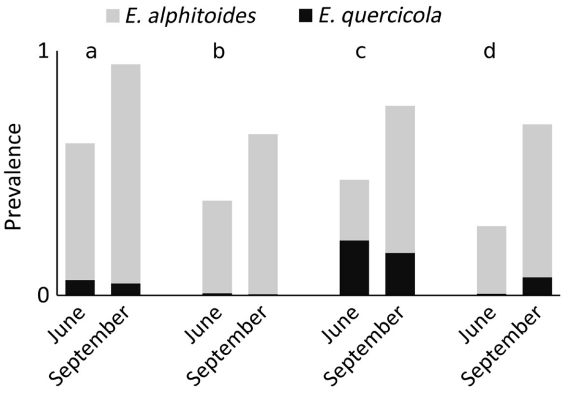

Fig. 2. Changes in the prevalence (percentage of oak seedlings infected) of *Erysiphe alphitoides* and *E. quercicola* during the growing season in four samplings: (a) mean values over 17 natural regenerations monitored in 2012; (b) mean values over 15 plantations monitored in 2012; (c) mean values over 23 natural regenerations monitored in 2013; (d) mean values over eight plantations monitored in 2013. The species prevalence was calculated as the product of disease prevalence observed in each stand (estimated from 30 seedlings) and identification of *Erysiphe* species in a sample of 10 infected leaves from different seedlings.

and from $nT + \tau$ to $(n+1)T$,

$$F((n+1)T) = \frac{\chi_1 F(nT+\tau)}{\chi_1 F(nT+\tau) + \chi_2(1-F(nT+\tau))},$$
$$I((n+1)T) = 1 - \exp(-[\chi_1 F(nT+\tau) + \chi_2(1-F(nT+\tau))]I(nT+\tau)). \quad (4)$$

We are interested in a coexistence equilibrium such that for all n after the equilibrium is reached,

$$F(nT) = F_0,\ I(nT) = I_0,\ F(nT+\tau) = F_\tau,$$
$$I(nT+\tau) = I_\tau, \text{ with } 0 < F_0, F_\tau, I_0, I_\tau < 1.$$

More specifically, the model has a limit cycle, and it is only the discrete-time part across years that has a fixed point.

Parameter estimation

The model was fitted on within season epidemic data; this allowed us to estimate secondary infection-related parameters (β_1, β_2, F_0). Assuming that species 1 and species 2 are at a coexistence equilibrium, we inferred between-season transmission coefficients (χ_1, χ_2) through equation (A.19) in Appendix S1: Section A.

Estimating parameters β_1, β_2 and initial condition $F(0) = F_0$ of model (3–4) was performed by fitting $F(t)$ to the data ($\{t_i\}$, $\{F_i\}$; Appendix S1: Table S1), given that $I(0) = I_0$ is known from the specific design of the first sampling date. Remembering that the initial proportion of infected young plants was 4×10^{-3} (in 2014), taking $I_0 = 1 \times 10^{-3}$ corresponds to assuming that each plant infection concerns one leaf over four in average. This is an upper bound. We will also consider $I(0) = I_0 = 4 \times 10^{-4}$ as a lower bound (i.e., 10% leaves initially infected). For 2014, the corresponding range is $4 \times 10^{-4} \leq I_0 \leq 1 \times 10^{-3}$, and for 2009, it is $5.6 \times 10^{-5} \leq I_0 \leq 1.4 \times 10^{-4}$. The final condition $F(\tau) = F_\tau$ will follow.

The vector of model parameters $\theta = (\beta_1, \beta_2, F_0)$ was estimated with the maximum-likelihood method assuming that each observation k_i, the number of leaves infected by species 1 at date t_i, is a realization of a binomial distribution of size m_i, the total number of single infections sampled at date t_i, and of probability of success $p_i(\theta) = F_\theta(t_i)$, the solution of model (3–4) at time t_i for a given θ. As independent leaves were observed at each sampling date, the likelihood is the product of the probability density of binomial distributions, that is,

$$\ell(\theta) = \prod_{i=1}^{n} \left[\binom{m_i}{k_i} F_\theta(t_i)^{k_i} (1 - F_\theta(t_i))^{m_i - k_i} \right] \quad (5)$$

Parameter inference was done independently for each data set with the "bbmle" package using the "nlminb" optimization routines of the R software environment (R Core Team 2015). Confidence intervals for model parameters were estimated using the function "profile" of the "bbmle" package. Ordinary differential Eqs. (3–4) were solved with the package "deSolve" using the function "lsoda" (Soetaert et al. 2010). Finally, a 95% confidence band was obtained for $F(t)$ by (1) sampling 1000 times in the multivariate normal distribution of $\hat{\theta}$, the maximum-likelihood estimator of θ, and (2) running the model (3–4) for each sampled value.

Results

Theory

Our main results are summarized in Figs. 3 and 4; the underlying analysis is provided in Appendix S1: Section A. Fig. 3 shows that coexistence is a relatively generic phenomenon in the model. Also, the coexistence region is generally narrower with increasing species similarity, that is, closer values of β and χ between the two species. For coexistence to occur, one species must have a greater secondary infection rate but a lower survival or primary infection rate than the other species. The greater the difference, the more likely coexistence may occur. Moreover, Fig. 3 shows that the reversal of species relative frequencies occurs in a significant part of the coexistence region. Last, Fig. 4 presents the dynamics of model (1–2) for a parameter set enabling coexistence together with species relative frequencies reversal.

Application

Table 2 reports estimated parameter values for both the lower and upper bound values of $I(0)$, to perform a sensitivity analysis to some uncertainty on initial incidence. This analysis was performed both for the 2009 and 2014 sampling campaigns in Cestas (Appendix S1: Tables S1 and S2). To estimate χ_1 and χ_2, we used equation (24) considering that F^*_τ as approximately equal to the asymptotic frequency of *E.a* relative to *E.q*. Indeed, rather than arbitrarily fixing a value to the season length τ, we made the weaker, sufficient, and reasonable assumption that τ is relatively large at the scale of the year (Jansen and Mulder 1999).

Fig. 5 presents the solutions obtained with parameters estimated for the 2009 and the 2014 data sets. As the curves corresponding to lower and upper bound values of $I(0)$ were in both cases almost indistinguishable, we only represented the solutions obtained for the lower bound values (i.e., $I(0) = 4 \times 10^{-4}$ for 2014, and $I(0) = 5.6 \times 10^{-5}$ for 2009). Incidentally, this implies that $I(0)$ is hardly identifiable with species relative frequencies data only. This is why we took advantage of available data on the initial infected plant density to determine the range of possible $I(0)$ values. However, the parameter estimates depended only marginally on the precise value of $I(0)$ (Table 2), except χ_1 and χ_2, whose ratio χ_2/χ_1 was relatively insensitive to $I(0)$ as well.

While secondary infection rates (β_1 and β_2) as well as the initial frequency of *E. alphitoides* relative to *E. quercicola* (F_0) were comparable between

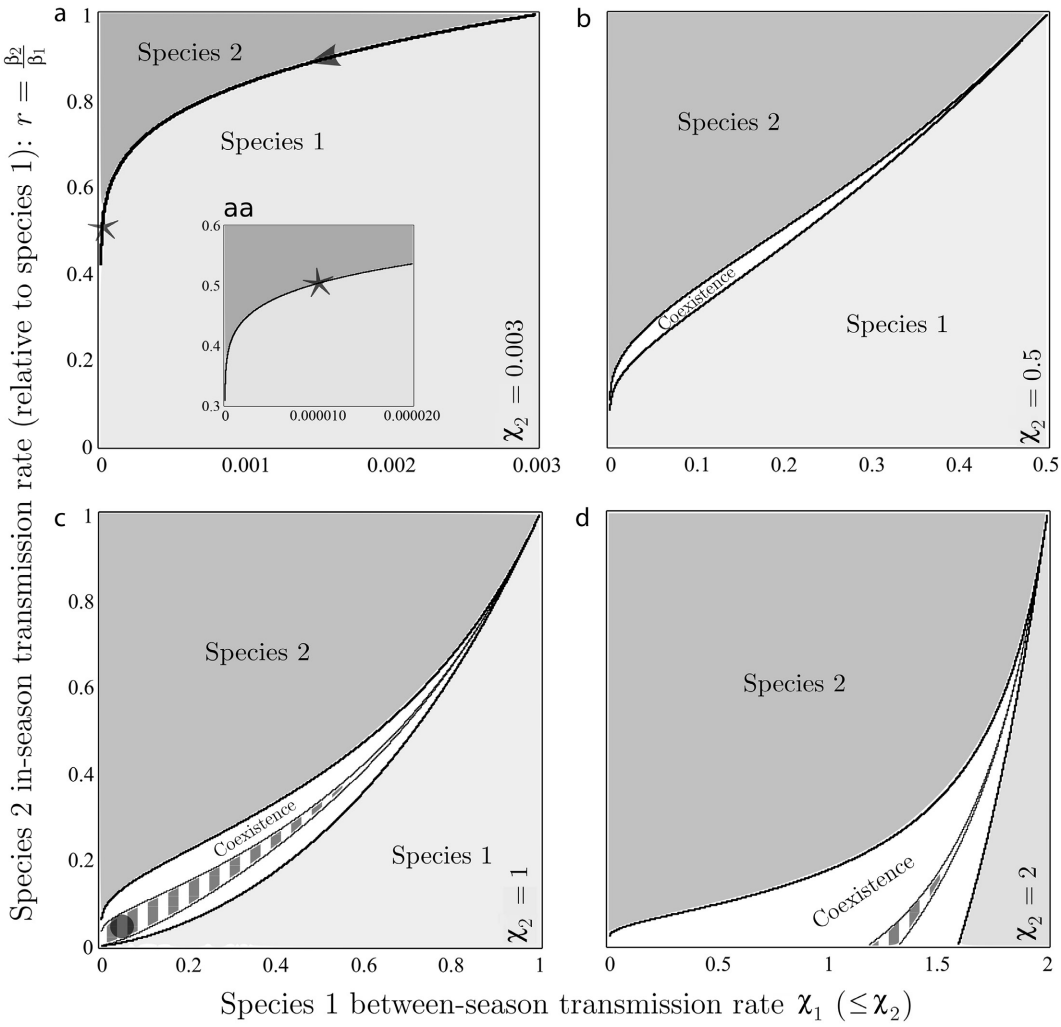

Fig. 3. Competitive exclusion or coexistence in the parameter space (χ_1, $r = \beta_2/\beta_1$) for several values of χ_2: (a) $\chi_2 = 0.003$, (b) $\chi_2 = 0.5$, (c) $\chi_2 = 1$, (d) $\chi_2 = 2$. We assumed $\alpha = 0$ and fast epidemiological dynamics compared with the length of the season. Under these assumptions, our results are independent on τ and on the values of β_1 and β_2 separately; it is indeed only the ratio $r = \beta_2/\beta_1$ that matters (Appendix S1: Section A). We also assumed $T = 1$ and $S_0 = 1$ without loss of generality. For instance, we may consider $\tau = 0.5$. The coexistence region is in white. Outside the coexistence region, either species 1 (bottom right side) or species 2 (upper left side) excludes the other species. (c–d) The hatched region inside the coexistence region corresponds to species relative frequencies reversal. For illustrative purposes, the hatched region is not represented in panel b. (a) The arrow along the coexistence curve indicates increasing species dissimilarity; the upper-right corner indeed corresponds to $\beta_1 = \beta_2$ and $\chi_1 = \chi_2$, that is, maximum species similarity, while the lower-left corner corresponds to $\beta_2 \ll \beta_1$ and $\chi_1 \ll \chi_2$, that is, maximum dissimilarity. The star denotes oak powdery mildew approximate location after parameter estimation (Table 2; 2014 data). (aa) Zoom on the * region. (c) The bullet shows the approximate location of the parameter set corresponding to Fig. 3.

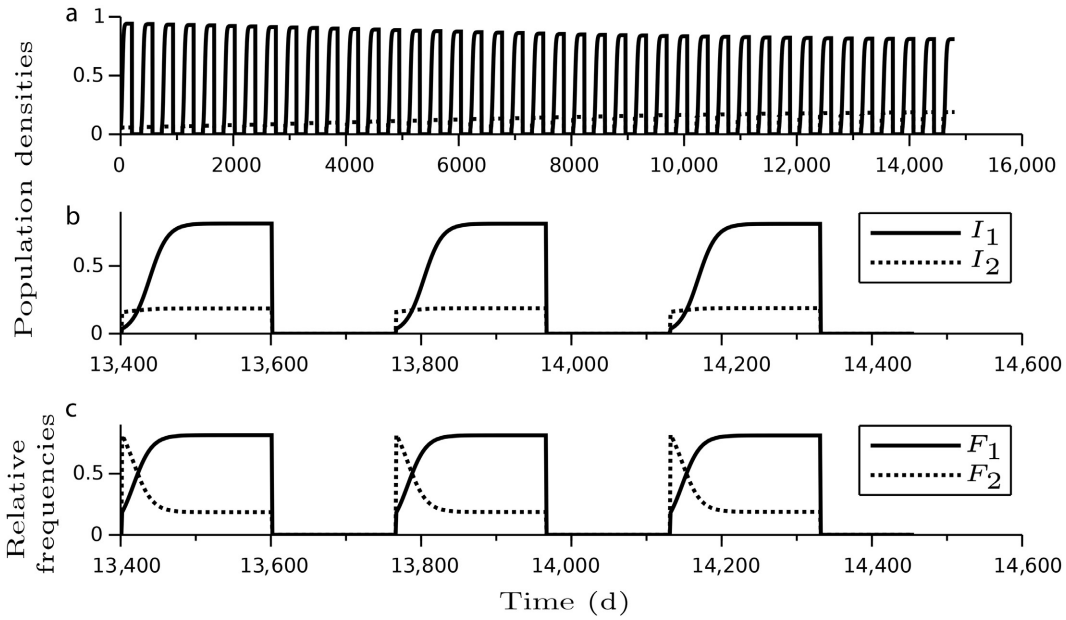

Fig. 4. Long-run coexistence with species relative frequencies reversal. Parameter values: $\alpha = 0$, $\beta_1 = 0.1$, $\beta_2 = 0.005$, $\chi_1 = 0.0493$, $\chi_2 = 0.96$, $T = 365$, $\tau = 200$, and $S_0 = 1$. (a) Infected densities I_1 and I_2, for $n = 40$ cycles (yr). (b) Zoom on the last three cycles. (c) Species relative frequencies over the last three cycles; that is, for $i = 1, 2$, $F_i = I_i/(I_1 + I_2)$.

2009 and 2014 studies, the survival and primary infection parameters (χ_1 and χ_2), which were very low for both years, may differ by an order of magnitude, as well as their ratio (χ_1/χ_2). As evidenced in Appendix S1: Fig. S1, it is also noteworthy that the 95% confidence ellipse in the plane (β_1, β_2) for the data set obtained in 2014 (with the more intensive monitoring) is fully included within the 95% confidence ellipse obtained in 2009 (with the less intensive monitoring).

As we have seen, coexistence for oak powdery mildew can be assumed from empirical evidence. Assuming that there is coexistence in the model, we found the most likely parameters for oak powdery mildew. Focusing on the more intensive monitoring (2014 data), we got $\chi_2 \approx 0.005$, $\chi_1 \ll 0.001$, and $r = \beta_2/\beta_1 \approx 0.5$. We therefore located the position of oak powdery mildew on Fig. 3a. This corresponds to nearly maximum species dissimilarity: *E. alphitoides* has a higher secondary infection rate, and a much lower between-season transmission parameter, than *E. quercicola*. The fact that for this specific value of χ_2 coexistence apparently occurs along a curve in the plane (χ_1, r) does not contradict the fact that coexistence is generic in the model. In the three-dimensional parameter space, the coexistence region has a significant volume. We get back to this point in the *Discussion*.

Table 2. Estimated parameter values on the within season epidemic dynamic of oak powdery mildew in 2009 and 2014.

Year	$I(0)$	β_1	β_2	F_0	F_τ	χ_1	χ_2	$r = \beta_2/\beta_1$	χ_1/χ_2
2014	1×10^{-3}	0.181	0.083	0.024	0.878	2.75×10^{-5}	0.008	0.458	3×10^{-3}
2014	4×10^{-4}	0.196	0.098	0.024	0.877	1.12×10^{-5}	0.003	0.5	3×10^{-3}
2009	1.4×10^{-4}	0.312	0.089	0.020	0.994	2.82×10^{-6}	0.025	0.287	1.1×10^{-4}
2009	5.6×10^{-5}	0.316	0.112	0.020	0.994	1.59×10^{-6}	0.010	0.344	1.5×10^{-4}

Notes: The vector of secondary infection-related parameters (β_1, β_2, F_0) was estimated by maximum likelihood for several values of the initial leaf density $I(0)$. Then, assuming that species 1 and species 2 are at coexistence equilibrium, we calculated between-season transmission coefficients (χ_1, χ_2) (see Appendix S1: Section A).

Discussion

First, we reported a new ecological finding: The reversal of the relative frequencies of the two species responsible for oak powdery mildew is recurrent across years. More specifically, we reported that species relative frequencies reversal occurred in 2014, which, combined with data from a previous study (Feau et al. 2012), provides original evidence that such a striking pattern repeats. Data were previously lacking to make a confident statement.

Second, we showed that the reversal of species relative frequencies can occur without compromising the long-term coexistence of the two species, which was a priori unintuitive. The recurrent reversal of species relative frequencies during the season is possible under slightly more restrictive conditions than coexistence alone. The reversal pattern might be interpreted as a lower ability of the species, which appears first in spring (*E. quercicola*) to colonize many seedlings during the season. This lower efficiency in secondary infections might be explained by differences in biological properties of conidia (acting as secondary inoculum) between the two species (which remains to be tested). In counterpart, overwintering in buds (as observed for *E. quercicola*) would provide a more efficient way to reinitiate epidemics in the following year than the production of chasmothecia (as observed for *E. alphitoides*).

Third, we showed that coexistence through temporal niche partitioning is biologically plausible, as it is a generic phenomenon from our model. This is a major advance compared with previous studies (Hamelin et al. 2011, Mailleret et al. 2012), where coexistence was only shown to be mathematically possible. That is, we showed that coexistence is not a mathematical singularity as it concerns a significant region of the three-dimensional parameter space (Fig. 3).

Last, we showed that the model satisfactorily fits the data and provides insights into the survival and transmission rates of the parasite species, as well as on their population dynamics. The adjusted seasonal dynamics are in remarkable agreement with a set of independent observations (Fig. 2). More specifically, we found that one species is likely present at a relatively low level throughout the season (*E. quercicola*), while the second (*E. alphitoides*) has a high multiplication rate during the season but has a low survival rate (Fig. 4).

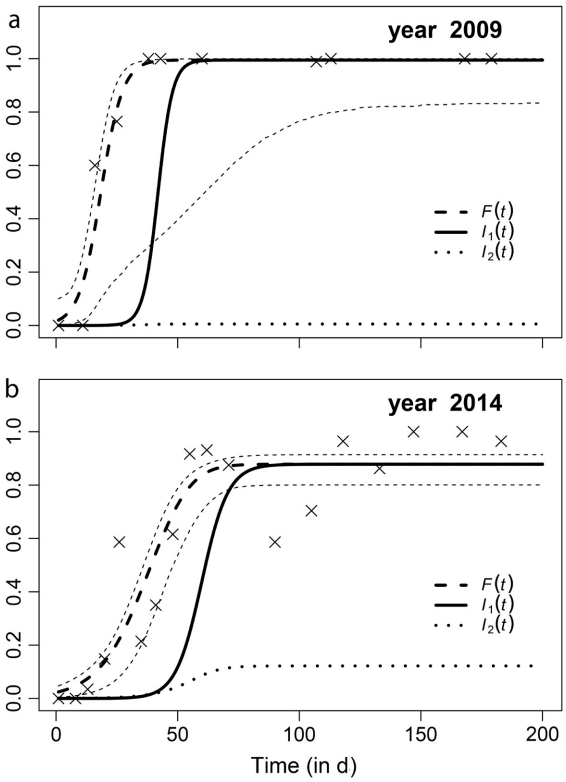

Fig. 5. Fitting model (3–4) to the data (crosses; Appendix S1: Tables S1 and S2) through a maximum-likelihood method. The bold dashed curve represents $F(t)$, the frequency of species 1 (*Erysiphe alphitoides*) relative to species 2 (*E. quercicola*); the thin dashed curves delimit a 95% confidence interval on $F(t)$. The bold solid and bold dotted curves represent inferred parasite population densities $I_1(t)$ (*E. alphitoides*) and $I_2(t)$ (*E. quercicola*), respectively. Parameter values: (a) $\beta_1 = 0.316$, $\beta_2 = 0.112$, $\chi_1 = 1.59 \times 10^{-6}$, $\chi_2 = 0.01$, (b) $\beta_1 = 0.196$, $\beta_2 = 0.098$, $\chi_1 = 1.12 \times 10^{-5}$, $\chi_2 = 0.003$ (Table 2).

Such an agreement between theory and observation is all the more surprising that several restrictions were made in developing the ecological model. Foremost among them was the restriction to a constant leaf (or resource) density all along the season. It would be interesting to relax this assumption and explore how parasite coexistence is impacted by intraseasonal host dynamics, although specifying host (e.g., oak) phenology would make the model less generic. Also, we assumed that the leaf removal rate

was zero for simplicity. Preliminary numerical explorations indicate that the coexistence region shrinks with increasing α values. This is likely because we considered that only individuals that are still infectious at the end of the season can contribute to parasite transmission to the next season through primary inoculum production. A more realistic but less tractable model would explicitly keep track primary inoculum production throughout the season (not only at the end of the season). Such an exploration is left for future research.

From a broader perspective, we showed that seasonal succession of two sibling parasite species responsible for oak powdery mildew provides one of the few examples of coexistence by temporal niche partitioning at the scale of the season, through exploitative competition.

Moreover, we were able to locate oak powdery mildew in the parameter space (Fig. 3a), indicating that *E. alphitoides* and *E. quercicola* achieve nearly maximum dissimilarity. Similarity generally narrows the coexistence region in the parameter space, as expected from the literature (MacArthur and Levins 1967, Bonsall et al. 2004, Barabás et al. 2012).

More puzzling is the fact that the coexistence region is quite narrow for parameter values corresponding to oak powdery mildew. This apparently implies that small phenotypic deviations should lead to competitive exclusion and the loss of coexistence. Moreover, one may wonder what is the probability that both species got, by chance, precisely the pair of phenotypes, which allow them to coexist. However, as we will see, phenotypic changes may be due to both exogenous factors or mutations, which complicates the picture.

First, exogenous factors (e.g., climate change, host adaptation) would in principle simultaneously impact both species parameters at the same time, so coexistence may not always be lost. For instance, multiplying the secondary infection rates β_1 and β_2 by some factor leaves $r = \beta_2/\beta_1$ unchanged: Such changes do not perturb coexistence. Similarly, simultaneous changes in the between-season transmission parameters χ_1 and χ_2 may not always result in the loss of coexistence, at least in the short run. Indeed, the region of near coexistence is also one where species could coexist for a long time. Actually, an alternative scenario that could explain the pattern that we observe is that the two species are near neutral in terms of coexistence and that in the very long run one species will outcompete the other, unless new arrivals replenish the slowly disappearing species (Bonsall et al. 2004, Scheffer and van Nes 2006). Second, mutations do not initially concern the whole population, but a small subset of the population. Whether the small mutant subpopulation can invade and replace the resident population, so that we can consider that the parameter corresponding to one species has changed, is not trivial. Based on the same model, Hamelin et al. (2011) showed that a mutation-selection process may lead one ancestral asexual species to segregate into two species diverging along a trade-off between in-season transmission (β) and off-season survival (χ). Both species ultimately coexist. Therefore, it may well be that the fine-tuning apparently required for coexistence to occur is actually the product of Darwinian evolution (Geritz et al. 2004).

Recent phylogenetic studies strongly suggest that *E. alphitoides* and *E. quercicola* evolved in sympatry from a common ancestor species pathogenic on an Asian *Quercus* (Takamatsu et al. 2007, 2015). The evolutionary divergence may have been driven by climate or host adaptation (Takamatsu et al. 2015). In particular, contrary to *E. alphitoides*, found only on deciduous oaks, *E. quercicola* seems to be better adapted to warmer climates and evergreen oaks (Takamatsu et al. 2015). Under these conditions, overwintering in buds could represent a lower-cost solution compared with overwintering as chasmothecia; thus, *E. quercicola* might have evolved a higher survival efficiency in buds. In the putative native area of both species in Japan, *E. quercicola* mostly produces flag shoots (although chasmothecia can rarely be observed), whereas numerous chasmothecia are found for *E. alphitoides* (S. Takamatsu, *personal communication*). The overwintering differences observed in the native area would have been kept in the introduced area (Europe), where up to now flag shoots have been strictly associated with *E. quercicola* and chasmothecia with *E. alphitoides*.

Overwintering differences might even have been exacerbated in relation with severe bottlenecks during introduction events. Most powdery mildew species are heterothallic, which means

that the production of chasmothecia (sexual structures) requires the encounter of mycelia from two different mating types. *E. quercicola*, which is less frequent in Europe (Mougou-Hamdane et al. 2010), might experience higher mate limitation than *E. alphitoides*. In particular, *E. quercicola* might still be affected by a highly unbalanced mating type ratio, challenging sexual reproduction, as is often observed in introduced plant pathogen populations (Raymond 1924, Day et al. 2004, Grünwald et al. 2012).

An interesting output of the model is that it could explain the coexistence of *E. quercicola* with *E. alphitoides* at a low density throughout the season, the relative decrease in *E. quercicola* being mostly a result of *E. alphitoides* buildup. From a more general point of view, our results suggest that the co-occurrence of parasite species in the same host might be explained first by "niche filtering" (drawing closely related species together, here in the same genus), as previously shown for some animal parasites (Mouillot et al. 2005) and other taxa (Fowler et al. 2014) then by dissimilarity within this species pool. It would be worth investigating more plant parasite complexes to support or refute this hypothesis, with a special attention to spatial scales (Mouillot et al. 2005).

Acknowledgments

The authors are very grateful to Gilles Saint-Jean and the technicians of the French Forest Health Department for field sampling, and to Damien Dezette and Marie Massot for molecular studies. The discussion benefited from interesting comments by Susumu Takamatsu. This work was supported by a grant overseen by the French National Research Agency (ANR) as part of the "Blanc2013" program (ANR-13-BSV7-0011, FunFit project). FMH also acknowledges funding from the French Institute for Research in Agriculture "Plant Health and the Environment" Division. We thank one anonymous reviewer for helpful suggestions.

Literature Cited

Adam, R., and K. Thibault. 2006. Temporal resource partitioning by bats at water holes. Journal of Zoology 270:466–472.

Albrecht, M., and N. Gotelli. 2001. Spatial and temporal niche partitioning in grassland ants. Oecologia 126:134–141.

Armstrong, R. A., and R. McGehee. 1980. Competitive exclusion. American Naturalist 115:151–170.

Barabás, G., S. Pigolotti, M. Gyllenberg, U. Dieckmann, and G. Meszéna. 2012. Continuous coexistence or discrete species? A new review of an old question. Evolutionary Ecology Research 14:523–554.

Bonsall, M. B., V. A. Jansen, and M. P. Hassell. 2004. Life history trade-offs assemble ecological guilds. Science 306:111–114.

Carothers, J. H., and F. M. Jaksić. 1984. Time as a niche difference: the role of interference competition. Oikos 42:403–406.

Castro-Arellano, I., and T. E. Lacher. 2009. Temporal niche segregation in two rodent assemblages of subtropical Mexico. Journal of Tropical Ecology 25:593–603.

Day, J., R. Wattier, D. Shaw, and R. Shattock. 2004. Phenotypic and genotypic diversity in *Phytophthora infestans* on potato in Great Britain, 1995–98. Plant Pathology 53:303–315.

Di Bitetti, M. S., Y. E. Di Blanco, J. A. Pereira, A. Paviolo, and I. J. Pérez. 2009. Time partitioning favors the coexistence of sympatric crab-eating foxes (*Cerdocyon thous*) and pampas foxes (*Lycalopex gymnocercus*). Journal of Mammalogy 90: 479–490.

Feau, N., A. Lauron-Moreau, D. Piou, B. Marçais, C. Dutech, and M.-L. Desprez-Loustau. 2012. Niche partitioning of the genetic lineages of the oak powdery mildew complex. Fungal Ecology 5:154–162.

Fitt, B. D., Y.-J. Huang, F. van den Bosch, and J. S. West. 2006. Coexistence of related pathogen species on arable crops in space and time. Annual Review of Phytopathology 44:163–182.

Fowler, D., J.-P. Lessard, and N. J. Sanders. 2014. Niche filtering rather than partitioning shapes the structure of temperate forest ant communities. Journal of Animal Ecology 83:943–952.

Gause, G. 1934. The struggle for existence. Williams and Wilkins, Baltimore, Maryland, USA.

Geritz, S. A., É. Kisdi, G. Meszéna, and J. A. J. Metz. 2004. Adaptive dynamics of speciation: ecological underpinnings. Pages 54–75 *in* U. Dieckmann, M. Doebeli, J. A. J. Metz, and D. Tautz, editors. Adaptive speciation. Cambridge University Press, Cambridge, UK.

Glawe, D. A. 2008. The powdery mildews: a review of the world's most familiar (yet poorly known) plant pathogens. Annual Review of Phytopathology 46:27–51.

Grünwald, N. J., M. Garbelotto, E. M. Goss, K. Heungens, and S. Prospero. 2012. Emergence of the sudden oak death pathogen *Phytophthora ramorum*. Trends in Microbiology 20:131–138.

Hamelin, F. M., M. Castel, S. Poggi, D. Andrivon, and L. Mailleret. 2011. Seasonality and the evolutionary divergence of plant parasites. Ecology 92: 2159–2166.

Harabiš, F., A. Dolnỳ, and J. Šipoš. 2012. Enigmatic adult overwintering in damselflies: coexistence as weaker intraguild competitors due to niche separation in time. Population Ecology 54:549–556.

Hardin, G. 1960. The competitive exclusion principle. Science 131:1292–1297.

Harrington, L. A., A. L. Harrington, N. Yamaguchi, M. D. Thom, P. Ferreras, T. R. Windham, and D. W. McDonald. 2009. The impact of native competitors on an alien invasive: temporal niche shifts to avoid interspecific aggression. Ecology 90:1207–1216.

Hayward, M. W., and R. Slotow. 2009. Temporal partitioning of activity in large African carnivores: tests of multiple hypotheses. South African Journal of Wildlife Research 39:109–125.

Hutchinson, G. E. 1961. The paradox of the plankton. American Naturalist 95:137–145.

Jansen, V. A., and G. Mulder. 1999. Evolving biodiversity. Ecology Letters 2:379–386.

Jones, M., Y. Mandelik, and T. Dayan. 2001. Coexistence of temporally partitioned spiny mice: roles of habitat structure and foraging behavior. Ecology 82:2164–2176.

Kermack, W. O., and A. G. McKendrick. 1927. A contribution to the mathematical theory of epidemics. Proceedings of the Royal Society of London A 115:700–721.

Kisdi, E. 2012. F1000Prime Recommendation of [Hamelin FM et al., *Ecology* 2011, 92(12):2159-66]. F1000 Prime.

Koide, R. T., D. L. Shumway, B. Xu, and J. N. Sharda. 2007. On temporal partitioning of a community of ectomycorrhizal fungi. New Phytologist 174:420–429.

Kronfeld-Schor, N., and T. Dayan. 2003. Partitioning of time as an ecological resource. Annual Review of Ecology Evolution and Systematics 34: 153–181.

Loreau, M. 1989. On testing temporal niche differentiation in carabid beetles. Oecologia 81:89–96.

MacArthur, R., and R. Levins. 1967. The limiting similarity, convergence, and divergence of coexisting species. American Naturalist 101:377–385.

Mailleret, L., M. Castel, J. Montarry, and F. M. Hamelin. 2012. From elaborate to compact seasonal plant epidemic models and back: Is competitive exclusion in the details? Theoretical Ecology 5:311–324.

Mailleret, L., and V. Lemesle. 2009. A note on semi-discrete modelling in the life sciences. Philosophical Transactions of the Royal Society of London A 367:4779–4799.

Marçais, B., and M.-L. Desprez-Loustau. 2014. European oak powdery mildew: impact on trees, effects of environmental factors, and potential effects of climate change. Annals of Forest Science 71: 633–642.

Morin, P. J. 2011. Community ecology. Second Edition. Wiley-Blackwell, Oxford, UK.

Mougou, A., C. Dutech, and M.-L. Desprez-Loustau. 2008. New insights into the identity and origin of the causal agent of oak powdery mildew in Europe. Forest Pathology 38:275–287.

Mougou-Hamdane, A., X. Giresse, C. Dutech, and M.-L. Desprez-Loustau. 2010. Spatial distribution of lineages of oak powdery mildew fungi in France, using quick molecular detection methods. Annals of Forest Science 67:212.

Mouillot, D., A. Šimková, S. Morand, and R. Poulin. 2005. Parasite species coexistence and limiting similarity: a multiscale look at phylogenetic, functional and reproductive distances. Oecologia 146: 269–278.

R Core Team. 2015. R: a language and environment for statistical computing. R Foundation for Statistical Computing, Vienna, Austria. https://www.r-project.org/

Raymond, J. 1924. Périthèces de *Microsphaera quercina* (Schw.) Burr observés dans le sud-ouest de la France. Revue de Pathologie Végétale et D'Entomologie Agricole 11:254–258.

Scheffer, M., and E. H. van Nes. 2006. Self-organized similarity, the evolutionary emergence of groups of similar species. Proceedings of the National Academy of Sciences 103:6230–6235.

Schoch, C. L., K. A. Seifert, S. Huhndorf, V. Robert, J. L. Spouge, C. A. Levesque, W. Chen, and Fungal Barcoding Consortium. 2012. Nuclear ribosomal internal transcribed spacer (ITS) region as a universal DNA barcode marker for Fungi. Proceedings of the National Academy of Sciences 109: 6241–6246.

Segarra, J., M. J. Jeger, and F. van den Bosch. 2001. Epidemic dynamics and patterns of plant diseases. Phytopathology 91:1001–1010.

Shimadzu, H., M. Dornelas, P. A. Henderson, and A. E. Magurran. 2013. Diversity is maintained by seasonal variation in species abundance. BMC Biology 11:98.

Soetaert, K. E. R., T. Petzoldt, and R. W. Setzer. 2010. Solving differential equations in R: package deSolve. Journal of Statistical Software 33:1–25.

Stuble, K. L., M. A. Rodriguez-Cabal, G. L. McCormick, I. Jurić, R. R. Dunn, and N. J. Sanders. 2013. Tradeoffs, competition, and coexistence in eastern

deciduous forest ant communities. Oecologia 171:981–992.

Takamatsu, S., U. Braun, S. Limkaisang, S. Kom-Un, Y. Sato, and J. H. Cunnington. 2007. Phylogeny and taxonomy of the oak powdery mildew *Erysiphe alphitoides* sensu lato. Mycological Research 111:809–826.

Takamatsu, S., H. Ito, Y. Shiroya, L. Kiss, and V. Heluta. 2015. First comprehensive phylogenetic analysis of the genus *Erysiphe* (Erysiphales, Erysiphaceae) I. The *Microsphaera* lineage. Mycologia 107:475–489.

Taylor, J. W., D. J. Jacobson, S. Kroken, T. Kasuga, D. M. Geiser, D. S. Hibbett, and M. C. Fisher. 2000. Phylogenetic species recognition and species concepts in fungi. Fungal Genetics and Biology 31: 21–32.

Valeix, M., S. Chamaillé-Jammes, and H. Fritz. 2007. Interference competition and temporal niche shifts: elephants and herbivore communities at waterholes. Oecologia 153:739–748.

Winder, M. 2009. Photosynthetic picoplankton dynamics in Lake Tahoe: temporal and spatial niche partitioning among prokaryotic and eukaryotic cells. Journal of Plankton Research 31:1307–1320.

Ziv, Y., Z. Abramsky, B. P. Kotler, and A. Subach. 1993. Interference competition and temporal and habitat partitioning in two gerbil species. Oikos 66: 237–246.

Supporting Information

Additional Supporting Information may be found online at: http://onlinelibrary.wiley.com/doi/10.1002/ecs2.1517/full